Catalog of PSDs in the solar wind

– solar max and min

Project acronym: *STORM*

Project title:

Solar system plasma Turbulence: Observations, inteRmittency and Multifractals

Grant Agreement number: *313038*

Coordinator: Belgian Institute for Space Aeronomy

Contact person: *Dr. Marius Echim*

Project co-funded by the European Commission,

Seventh Framework Programme

Funding Scheme: *FP7-SPACE-2012-1, Collaborative Project*

Due date of deliverable:	**Month 12**
Actual submission date:	**February 15, 2014**
Start date of the project:	**January 1, 2013**
Project duration:	**3 years**

List of contributing authors:

Ilpo Virtanen, UOulu
Kalevi Mursula, UOulu
Pauli Väisänen, UOulu
Marius Echim, IASB
Hervé Lamy, IASB
Giuseppe Consolini, INAF
Roberto Bruno, INAF
Giuseppe Pallocchia, INAF
Emilya Yordanova, IRF
Peter Kovacs, MFGI
Costel Munteanu, INFLPR-ISS
Eliza Teodorescu, INFLPR-ISS
Gabriel Voitcu, INFLPR-ISS
Wieslaw Macek, SRC
Anna Wawrzaszek, SRC

TABLE OF CONTENTS

1. Introduction

2. Data sources, satellites and data intervals during solar minimum and maximum conditions

3. Data processing and preparation for PSD analysis

4. Solar wind and IMF parameters from the different satellites

4.1 Ulysses data

4.2. Cluster solar wind data

4.3 Venus Express solar wind data

5. Properties of solar wind and IMF during solar minimum and maximum conditions

6 Selection of data intervals of high and slow solar wind

6.1 Ulysses

6.2 Cluster

6.3 Venus Express

7. The Welch method for PSD calculation

8. Spectral properties of turbulence in the solar wind from PSD analysis

9. A catalog of PSD in the solar wind

10. Some relevant examples of PSDs

11. References

Deliverable 2.1 Catalog of PSDs in the solar wind – solar max and min

1. Introduction

The Work package 2 of the FP7 project STORM is devoted to the analysis of intermittent turbulence in the solar wind. This work package provides on the one hand a quantitative description of turbulence, of its inertial range and the properties of the energy transfer between scales and on the other hand an estimation of turbulence upstream of the outer layers of the planetary plasma environment – an input for space weather events in case of the Earth. This deliverable focus on the analysis of the power spectral density of the turbulent fluctuations in the solar wind at various radial distances and various helio-latitudes, during the minimum and maximum of the solar cycle. The data bases to be used are provided by the core missions of STORM: Ulysses, Cluster and Venus Express.

The power spectrum of turbulent fluctuations is characterized by: (1) the driving range at largest scales – the source of the energy “cascading” to smaller scales; (2) the dissipation range at smallest scales where the turbulence energy is dissipated; (3) the inertial range at the intermediate scales the energy cascade is often identified as a power law. The deliverable D2.1 contributes to STORM objectives as declared in the Grant Agreement:

- *“ To improve the physical insight on turbulence by investigating the topology of the energy transfer in the solar wind(in the ecliptic plane and at higher latitudes), .[..] ,and to search for quantitative measures for wave dispersion and/or coherent structures interaction;*
- *To improve the understanding of the dissipation mechanisms, in the solar wind [...] and search evidence for coherent structure dissipation versus wave damping*
- *To investigate the solar cycle effects on the energy cascade and dissipation mechanisms, in the solar wind [...] “*

The Deliverable 2.1 provides a catalog of power spectral densities (PSD) in the solar wind during selected solar maximum and minimum times. We have constructed an ftp archive containing electronic images of PSD of magnetic field and solar wind – at solar maximum and solar minimum for slow and fast solar wind. The ftp archive also contains the original data and the standardized data used for calculating the PSDs.

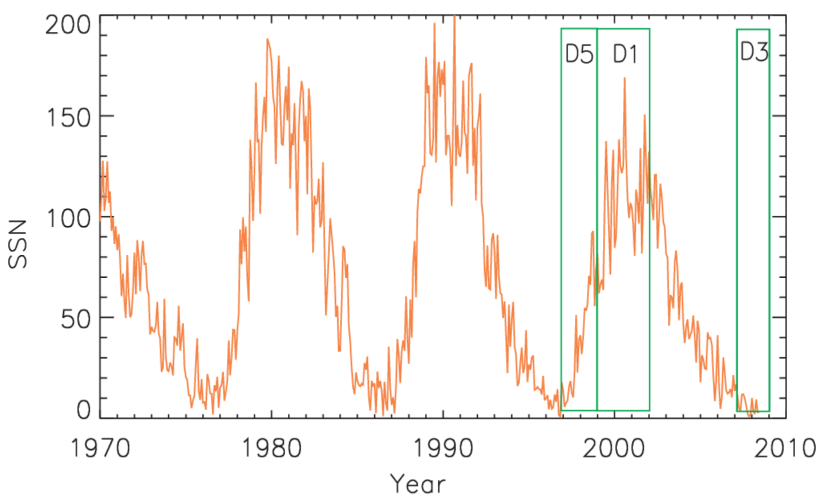

Figure 2.1: Sunspot numbers (SSN) in 1970–2010 and the three data intervals.

2. Data sources and time intervals during solar minimum and maximum conditions

As stated in the Grant Agreement, the analysis of solar wind data focuses on three time intervals: two of them, 1997-1998 and respectively 2007-2008 correspond to the solar minimum and the third one, 2000-2001 corresponds to solar maximum. The three time intervals define the databases D5MINSW (1997-1998), D3MINSW (2007-2008) and respectively D1MAXSW (1999-2001). D5MINSW includes data only from Ulysses; D1MAXSW includes data from Ulysses and in 2001 also from Cluster. During the second minimum time period, D3MINSW, there are data available from Ulysses, Cluster and Venus Express. Figure 2.1 shows these three time periods and their relation to sunspot activity.

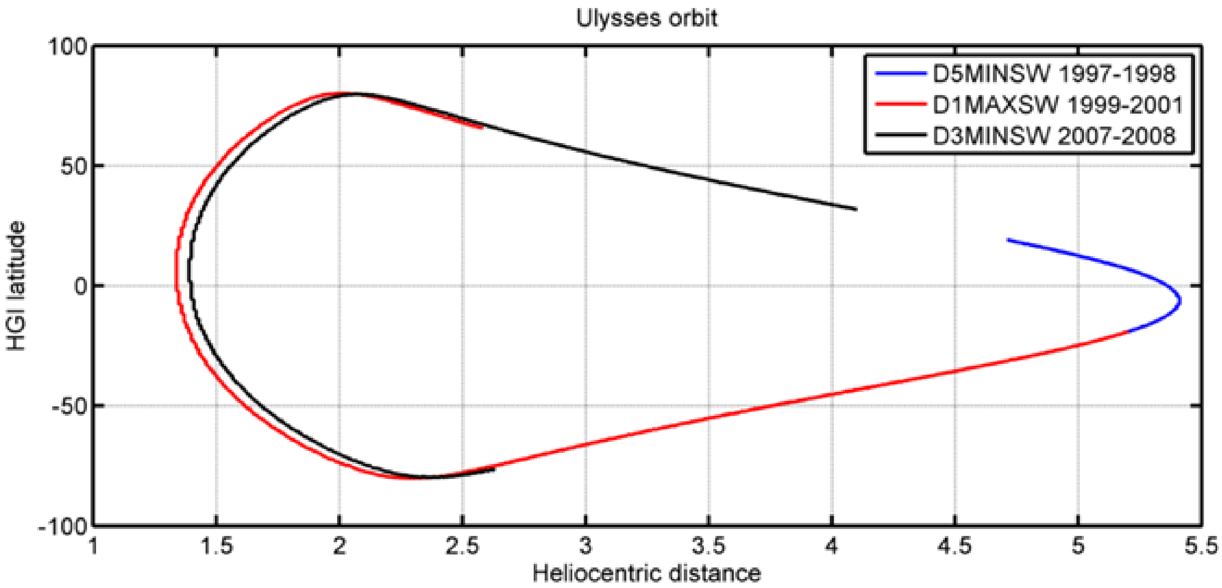

Figure 2.2 Ulysses orbit in heliographic coordinates (distance, latitude), during the three time periods. Note that they cover quite different heliospheric regions.

During its life time in 1992 – 2008 Ulysses completed three orbits around the Sun in a roughly polar orbit. The orbit perihelion (aphelion) is located in the solar equatorial plane at the distance of about 1.3 AU (5.4 AU). Ulysses was constantly in the solar wind but data selection is needed in order to separate "pure" fast and slow speed solar wind periods, as explained in Section 6. During the solar minimum, between 2007 – 2008, Ulysses data are indeed unique since the spacecraft was mainly measuring fast solar wind originating from the large polar coronal holes. An illustration of Ulysses orbit is given in Figures 2.2 and 2.3. Ulysses magnetic field and solar wind data are provided by ESA's Ulysses final archive (http://ufa.esac.esa.int).

ESA's Cluster satellite quartet was launched in 2000, and data are available from the beginning of 2001. Due to its highly eccentric orbit Cluster surveys the solar wind along a segment of the trajectory; the time spent by Cluster in the solar wind varies with the orientation of the orbit apogee, being longer when the apogee is close to the Earth-Sun axis. The time intervals when Cluster measured "in-situ" the solar wind properties were identified for 2001 and 2007 - 2008 and the corresponding data (magnetic field at high resolution and plasma variables) were added to the databases D1MAXSW and respectively D3MINSW. The solar wind data intervals from Cluster were organized as a function of the solar wind type: fast and slow . The details of the selection criteria are

explained in Section 6 of this report. Cluster data are provided by ESA's Cluster Active Archive (CAA, http://caa.estec.esa.int).

Venus Express (VEX) is a small spacecraft launched by the European Space Agency in 2005. VEX arrived at Venus in April 2006 when it started to send data measured in the complex Venusian environment. The spacecraft is equipped with instruments for the investigation of the neutral atmosphere, the ionosphere, the magnetosphere and the interaction with the solar wind: ASPERA (Analyser of Space Plasma and Energetic Atoms, Barabash et al., 2007) and MAG (Venus Express Magnetometer, Zhang et al., 2006) are the experiments relevant for STORM. An illustration of VEX spacecraft and its scientific instrumentation and of VEX orbit is illustrated in figure 4.1.

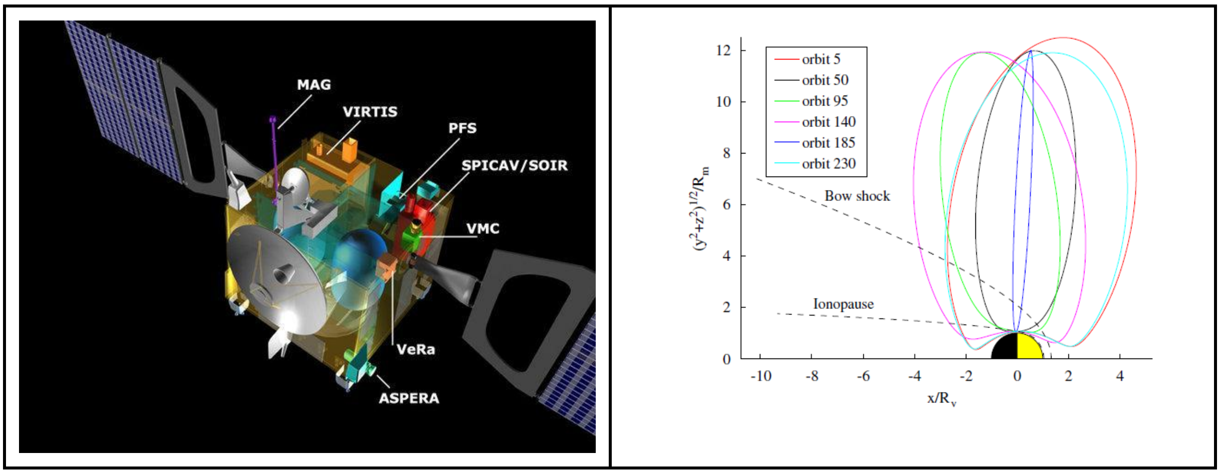

Figure 4.1. Illustration of the VEX spacecraft and its scientific instruments (picture courtesy of http://esa.int). Right: examples of some VEX orbits from 2006, soon after Venus insertion, and schematic illustration of Venus ionopause and bow shock positions (Barabash et al, 2007); note the long time periods when VEX is in the solar wind.

Venus Express (VEX) provides magnetic field and plasma measurements in the solar wind at Venus orbit at about 0.72 AU from the Sun. The magnetic field is measured on board VEX at high resolution (32 Hz), however calibrated data are available at 1 Hz (T. Zhang, private communication). Venus Express data are provided by the European Space Astronomy Center and ESA's Planetary Science Archive (http://www.rssd.esa.int/). We have been also in contact with the PI of the magnetometer experiment, Dr. Tielong Zhang from IFW Graz. The time intervals with possible windows of conjunction between Ulysses, Cluster and Venus Express are particularly interesting. VEX contributes magnetic field data to the , D3MINSW solar wind data base, at solar minimum.

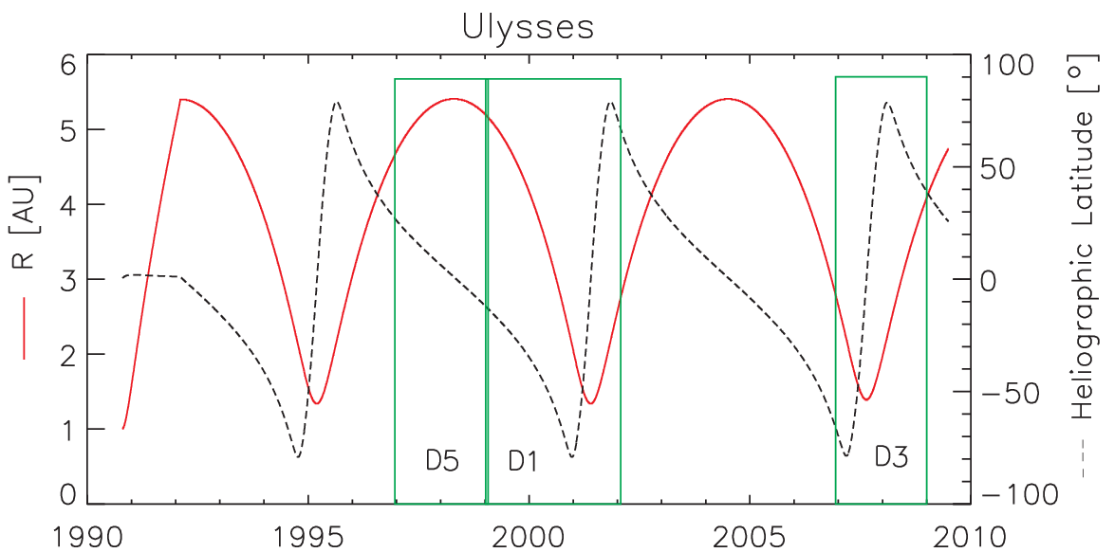

Figure 2.3: The heliographic latitude (continuous red line) and the heliocentric distance from the Sun (dashed black line) during while the Ulysses mission. The three time intervals are denoted in green.

3. Data pre-processing and preparation for PSD analysis

Ulysses magnetic field data (Balogh et al., 1992) in Ulysses final archive (http://ufa.esac.esa.int) are given in daily ASCII files with each data row including the following information (columns):

1 year
2 day of year
3 hour of day
4 minute of hour
5 second of minute
6 Radial component (RTN system) of vector magnetic field in nT
7 Transverse component (RTN system) of vector magnetic field in nT
8 Normal component (RTN system) of vector magnetic field in nT
9 Scalar magnitude of magnetic field in nT

Similarly, Ulysses plasma data (Bame et al., 1992) in the same archive contains the following information (columns):

1 year
2 day of year
3 hour of day
4 minute of hour
5 second of minute
6 sun-spacecraft distance in AU
7 heliospheric latitude of Ulysses in degrees
8 heliospheric longitude (Carrington longitude of Ulysses)

9 proton number density in particles per cubic centimeter
10 alpha number density in particles per cubic centimeter
11 proton temperature in Kelvin (large)
12 proton temperature in Kelvin (small)
13 Radial component (RTN system) of plasma velocity in km/sec
14 Tangential component (RTN system) of plasma velocity in km/sec
15 Normal component (RTN system) of plasma velocity in km/sec
16 Data quality condition flag

The RTN (Radial-Tangential-Normal) coordinate system is defined as follows: the R coordinate points radially away from the Sun through the spacecraft, T is determined by the cross product of R with the solar rotation axis and N is determined by the cross product of R and T.

The Ulysses data are partly unevenly sampled and there are also longer data gaps in each of the three time intervals studied. We use Matlab Welch algorithm to calculate power spectral densities. Therefore the data have to be resampled to constant resolution before further analysis. Matlab " "interp1" function is used as a resampling tool for Ulysses data. For data gaps in both Ulysses and Cluster data we use a linear interpolation method. (On the other hand, e.g., spline interpolation seems to produce some artefacts at the low-frequency end of the spectrum). Note that Cluster has several intervals with 100% data coverage, for which no interpolation was necessary.

Cluster data are available in CDF-format on the CAA web server (http://caa.estec.esa.int) that allows selection of data packages for the time intervals of interest for STORM. CDF file includes extensive information about data; in this study we only use the time, the three components of the magnetic field and the solar wind radial velocity.

Venus Express magnetic field data at 1 Hz resolution are structured as daily ASCII files, with the extension TAB; the data are organized in folders corresponding to each month of the year. Each file contains an introductory section of meta data with detailed information about the mission, the instrument, the spacecraft position in different coordinates and the time interval, along with detailed description of the measurements stored in the file. Each magnetic field data file contains nine columns corresponding to the following measurements:

- UTC time of observation, given as YYYY-MM-DDTHH:MM:SS.FFF
- 4 columns for the magnetic field data in Venus Solar Orbital (VSO) coordinates in nT.
  - B_x, B_y and B_z components
  - total magnetic field, B
- 4 columns for the spacecraft position in Venus Solar Orbital (VSO) coordinates in kilometers
  - X, Y and Z components
  - total distance, R

The VSO coordinate system is basically the Geocentric Solar Ecliptic system (GSE) generalized for

Venus. The X-axis points from the planet to the Sun, the Y-axis points in the opposite direction to the planetary motion and the Z axis is perpendicular to Venus orbital plane around the Sun.

The erroneous data are flagged with the value 99999.999. During the analysis, such values are removed from the time series which leads to uneven spacing of the measurements but we limit such data-gaps to a maximum of 30 seconds, which at 1 Hz resolution is equivalent to 30 consecutive missing measurements.

In the case of long data gaps it is impossible to calculate a reliable PSD even from the resampled data. We have excluded all such problematic periods after careful manual check. However, it is not reasonable to define exact limitations for data coverage or for the maximum data gap length allowed because of the many different types of gaps.

We have removed outliers from the Ulysses data manually. In case of Cluster plasma data, all values that are not within the limits of the respective solar wind type (fast: from 450-900 km/s; /slow 250-450 km/s) are removed as outliers. All removed outliers are listed in separate files available (see later). Note that for all data sets, the outliers form only a very small fraction of all data. Outliers were not removed from Cluster and Venus Express data.

Before PSD calculation we have removed from Ulysses and Cluster data the linear trend over the analyzed time interval, as well as the mean of the data. We have also divided the data by its standard deviation. As result, we have data with no linear trend, zero mean and variance equal to one.

4. Solar wind and IMF parameters from the STORM core missions

4.1 Ulysses data

In this study we use Ulysses magnetic field data from VHM-FGM magnetometer at 0.5 Hz and plasma data from from Ulysses SWOOPS at 8 minute resolution. A summary of Ulysses data parameters and their resolution is given in Table 4.1.

Table 4.1: Solar wind and interplanetary magnetic field (IMF) parameters selected for calculation of PSD from Ulysses database.

Parameters	Instrument	Data resolution
Radial velocity in km/sec	SWOOPS (Solar Wind Observations Over the Poles of the Sun)	original res.: 4 min, 8 min used res.: 8 min
Radial component of vector magnetic field in nT	VHM-FGM (Vector Helium Magnetometer / Flux Gate Magnetometer)	original res.: 1 s, 2 s used res.: 2 s

Transverse component of vector magnetic field in nT	VHM-FGM	original res.: 1 s, 2 s used res.: 2 s
Normal component of vector magnetic field in nT	VHM-FGM	original res.: 1 s, 2 s used res.: 2 s
Scalar magnitude of magnetic field in nT	VHM-FGM	original res.: 1 s, 2 s used res.: 2 s

4.2. Cluster data in the solar wind

The time intervals when Cluster was in the solar wind were selected close to the orbit apogee, between February and April 2001 and added to the D1MAXSW data base for solar maximum. Time intervals close to the Cluster apogee between January and April 2007 and respectively between January and April 2008 were added to the D3MINSW database for solar minimum.

The selection of Cluster solar wind intervals is based on the simultaneous scanning of the following parameters: spacecraft position, magnetic field magnitude (Balogh et al., 1997), ion velocity, omni-directional ion energy flux (Reme et al., 1997) and wave energy density (see Table 4.2, Decreau et al., 2001). A detailed description of selection criteria is given in section 6. The minimal length of an interval is 1 hour.

Table 4.2: Instruments and parameters used to select Cluster solar wind intervals.

Instrument	Quantity	Sampling rate	Parameter
AUX	Spacecraft position	60 s	$\mathbf{X}_{GSE}$, R_E
FGM	Magnetic field	0.0446s	$\|\mathbf{B}_{GSE}\|$, nT
CIS-HIA	Ion velocity	4 s	$\|\mathbf{V}_{GSE}\|$, km/s
CIS-HIA	Particle energy flux	4 s	$\mathbf{F}_E$, keV cm^{-2} s^{-1} sr^{-1} keV^{-1}
WHISPER	Wave form energy	0.2 s	$\mathbf{E}$, V^2 m^{-2} Hz^{-1}

4.3 Venus Express data in the solar wind

VEX-MAG provides measurements of the three components of the magnetic field with the resolution varying between 1 Hz (solar wind mode), 16 Hz (cruise mode) and 128 Hz (burst mode; Zhang et al., 2006). ASPERA provides measurements of the electron and ion spectra, their moments (density, temperature, velocity) as well as energetic neutral atom spectra (Barabash et al., 2007). MAG and

ASPERA are the instruments that provide data relevant for studies of space plasma turbulence. A summary of these parameters is included in Table 4.3. ESA maintains a data base that includes raw and calibrated data from all VEX experiments. Plasma and magnetic field data are also available from the French Automated Data Base Analysis (AMDA) website (http://amda.cdpp.eu). Due to the highly eccentric orbit, Venus Express spends most of the orbital time in the solar wind and therefore provides valuable data for turbulence studies. Moreover, in 2007-2008, the time interval included in the D3MINSW database, there is an inferior conjunction between Venus and Earth (VEX and Cluster), between July and August 2007.

Table 4.3. Parameters used from VEX MAG and ASPERA instruments.

Instrument	**Quantity**	**Sampling rate**	**Parameter**
	Spacecraft position	60 s	$\mathbf{X}_{VSO}$, R_V
MAG	Magnetic field	1 s, 1/32 s, 1/128 s	$\mathbf{B}_{VSO}$, nT
ASPERA	SW and planetary ion velocity	196 sec	$\lvert \mathbf{V}_{VSO} \rvert$, km/s
ASPERA	SW and planetary ion density	196 sec	n_p, cm^{-3}
ASPERA	Ion, electron energy flux	ion, 196 sec electron, 32 sec	$\mathbf{F}_E$, keV cm^{-2} s^{-1} sr^{-1} keV^{-1}

5. Properties of solar wind and IMF during solar minimum and maximum conditions

At solar minimum there are typically two large polar coronal holes, one in each solar hemisphere. During the solar minimum in mid-1990s the heliospheric (interplanetary) magnetic field from the northern polar coronal hole was oriented away from the Sun and the field from the southern coronal hole toward the Sun. The magnetic polarity reverses during maxima and it was oppositely oriented during the solar minimum in the 2000s. During solar minimum the fast solar wind streaming from polar coronal holes dominates at high latitudes. The fast solar wind observed during solar minima at low latitudes originates from the extension of polar coronal hole towards the solar equator. Measurements by Ulysses showed that the slow and the fast wind are two separate populations, whose velocity distributions peak at about 430 km/s and 760 km/s [*Erdös and Balogh, 2012*].

At solar maximum the coronal holes can be observed at any latitude and streams of fast and slow wind alternate all over the heliosphere. Nevertheless, the coronal holes are significantly smaller than at solar minimum. The peak values of the solar wind velocity tend to be smaller.

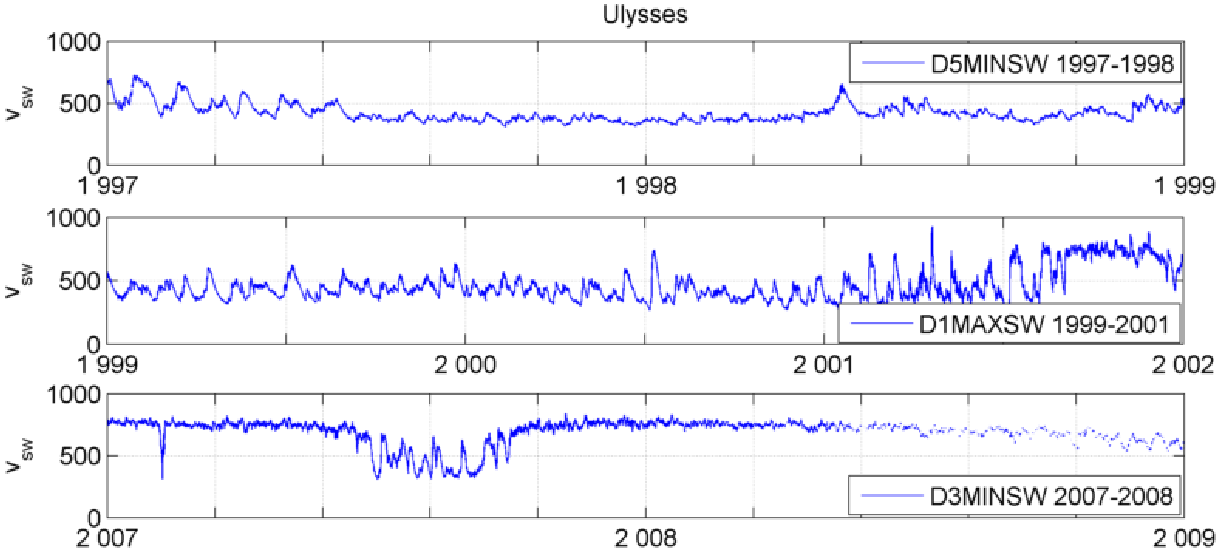

Figure 5.1: Solar wind velocity observed by Ulysses in 1997 - 1998, 1999 - 2001 and 2007 – 2008

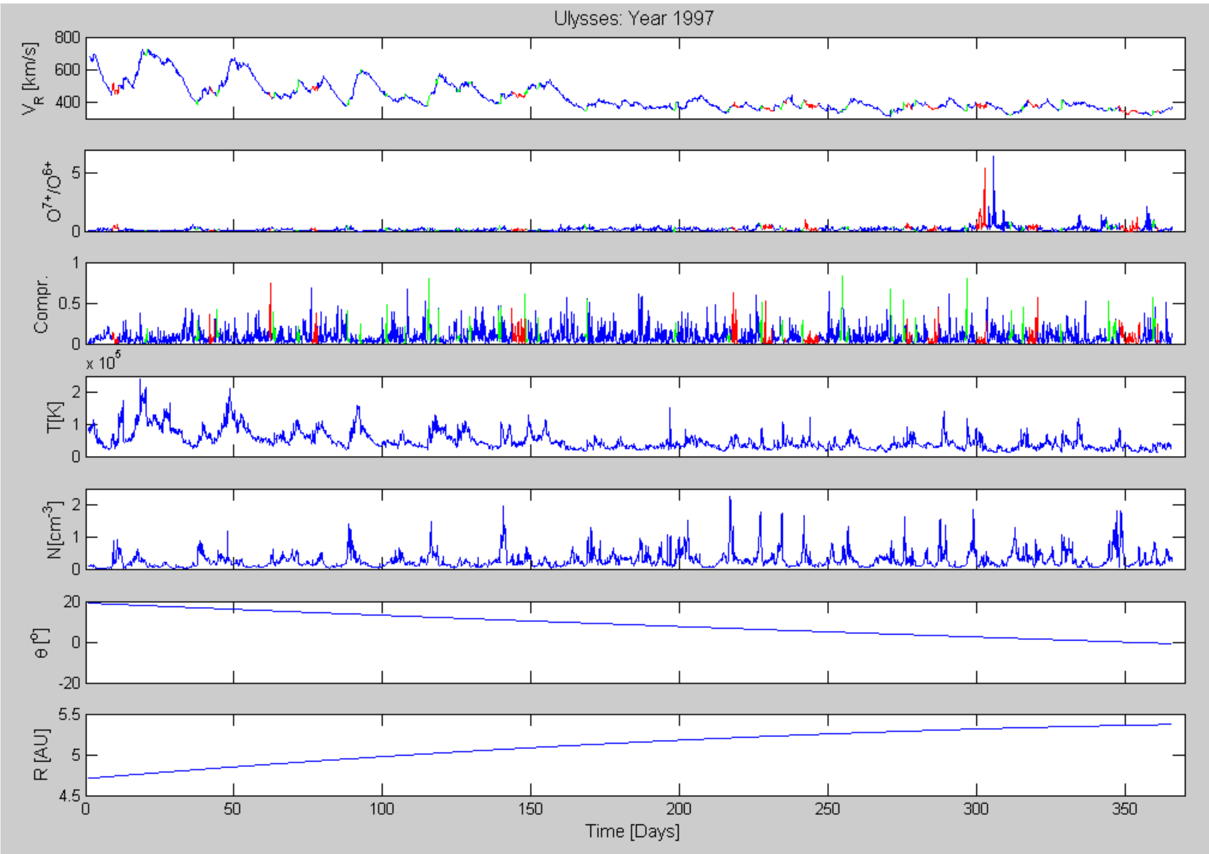

Figure 5.2: Selected parameters of solar wind and Ulysses position in 1997 (6-hour averages): solar wind speed, O^7/O^6 ratio, IMF compressibility, proton temperature, proton density at Ulysses, proton density scaled to 1 AU, heliographic latitude and radial distance of Ulysses. Red (green) color denotes the occurrences of a major CME (interplanetary shock, respectively).

The properties of the solar wind and the heliospheric magnetic field changed significantly between the last solar minima, in 1990s and 2000s. Magnetic fields in the solar photospheric polar regions [*Wang et al., 2009*] and polar coronal holes (observed in the heliosphere) dropped to a lower level [*Smith and Balogh, 2008*]. Also, the solar wind from polar coronal holes became less dense [*McComas et al., 2008*].

Figure 5.1 depicts the solar wind speed observed by Ulysses during the time intervals defined for the three STORM databases. Figures 5.2 – 5.4 show several parameters of the solar wind and the Ulysses position for one year of each of the three databases. In 1997 – 1998 Ulysses was at low latitudes close to the apogee (see Figure 2.3) and therefore it mostly observed slow wind. Between 1999 – 2001 Ulysses was flying over a wide latitude range in solar maximum conditions and it observed a few sectors of high speed streams but mainly slow wind. In 2007 – 2008 the probe completed the last fast latitude scan from south to north and observed mainly fast wind from the large polar coronal holes. (Note also that data from 15th of January 2008 onward the data is too poorly sampled for PSD calculation and will not be used here).

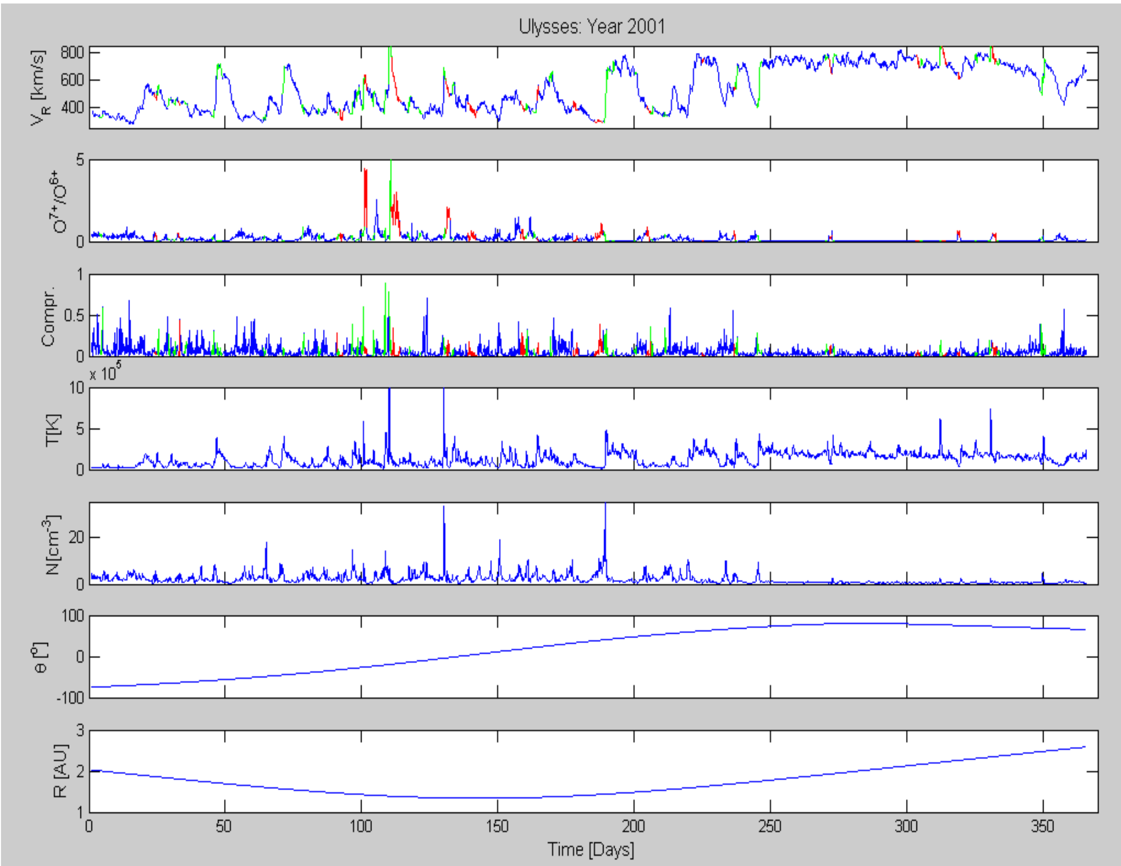

Figure 5.3: Selected parameters of solar wind and Ulysses position in 2001 (6-hour averages): the panels have the same structure as in figure 5.2.

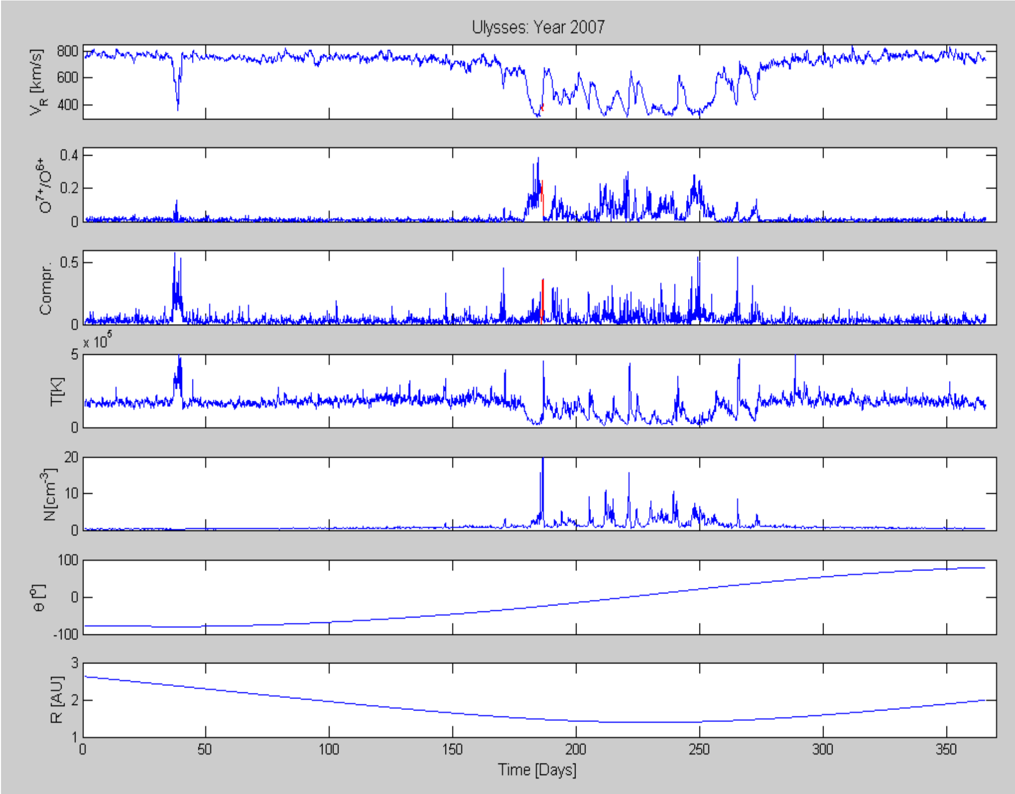

Figure 5.4: Selected parameters of solar wind and Ulysses position in 2007 (6-hour averages): the panels have the same structure as in figure 5.2.

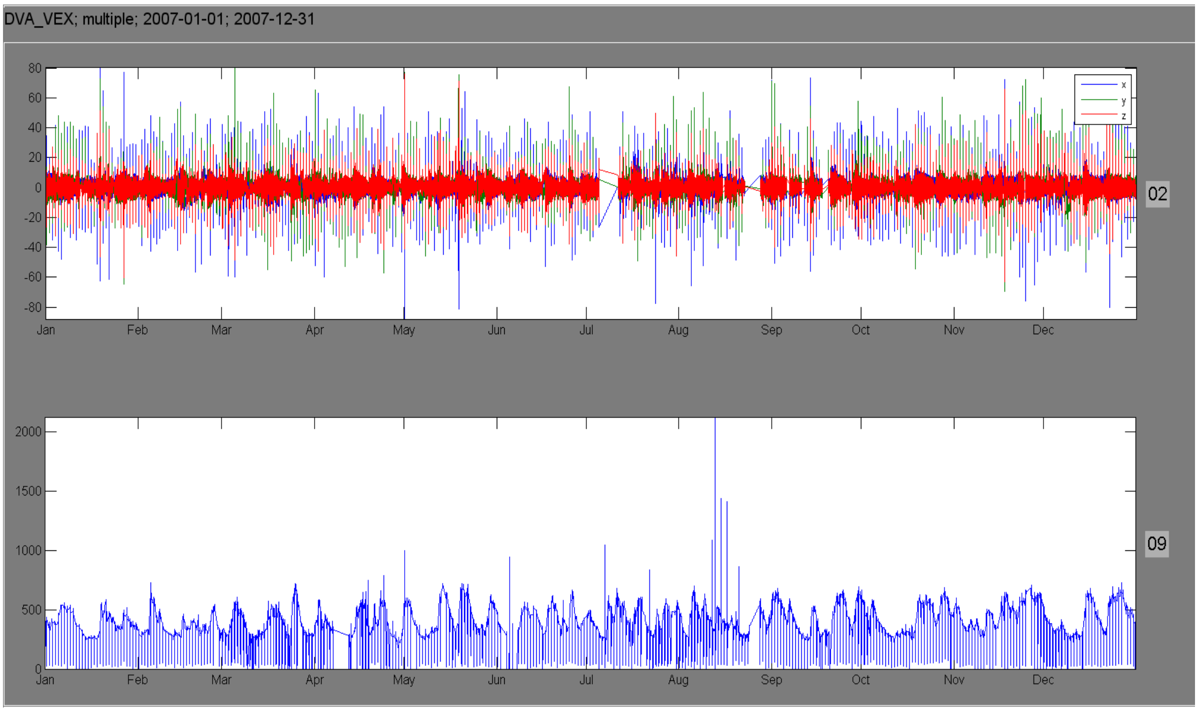

Figure 5.5. Summary plot of raw magnetic field (upper panel) and raw plasma bulk velocity (lower panel) measured by Venus Express in 2007. Note that the peak values of the velocity correspond to observations of high speed streams in the solar wind; the peaks of the magnetic field data identify crossings of the induced magnetosphere.

6 Selection of data intervals of high and slow solar wind

6.1 Ulysses

The main objective of Ulysses data survey and selection is to identify the two “pure” states of the solar wind, slow and fast. The data selection is made based on the analysis of 5 solar wind parameters:

- The radial velocity ,
- The Oxygen ion ratio O^{7+}/O^{6+},
- The magnetic Compressibility factor, i.e., $\frac{<|B|^2>-<|B|>^2}{(<B_R{}^2>-<B_R>^2)+(<B_T{}^2>-<B_T>^2)+(<B_N{}^2>-<B_N>^2)}$,
- The proton density n_p
- The proton temperature T_p

We have checked the literature (Yordanova et al., 2009; Lepri et al., 2012, Bruno and Carbone, 2013) and we defined a set of criteria and thresholds to identify the solar wind type and origin, i.e. fast and slow wind originating in the polar coronal holes and respectively the streamer belt. One individual criterion and threshold was assigned to each of the 5 solar wind parameters shown above. These criteria and thresholds are shown in Figure 6.1 and in Table 6.1. Interplanetary transients like CMEs and shocks were excluded from the analysis. A list of such transients encountered by Ulysses between 1992 and 2008 was published by Gosling and Reisenfeld (2002) and Gosling and Ebert (2008) (see http://swoops.lanl.gov/cme_list.html)

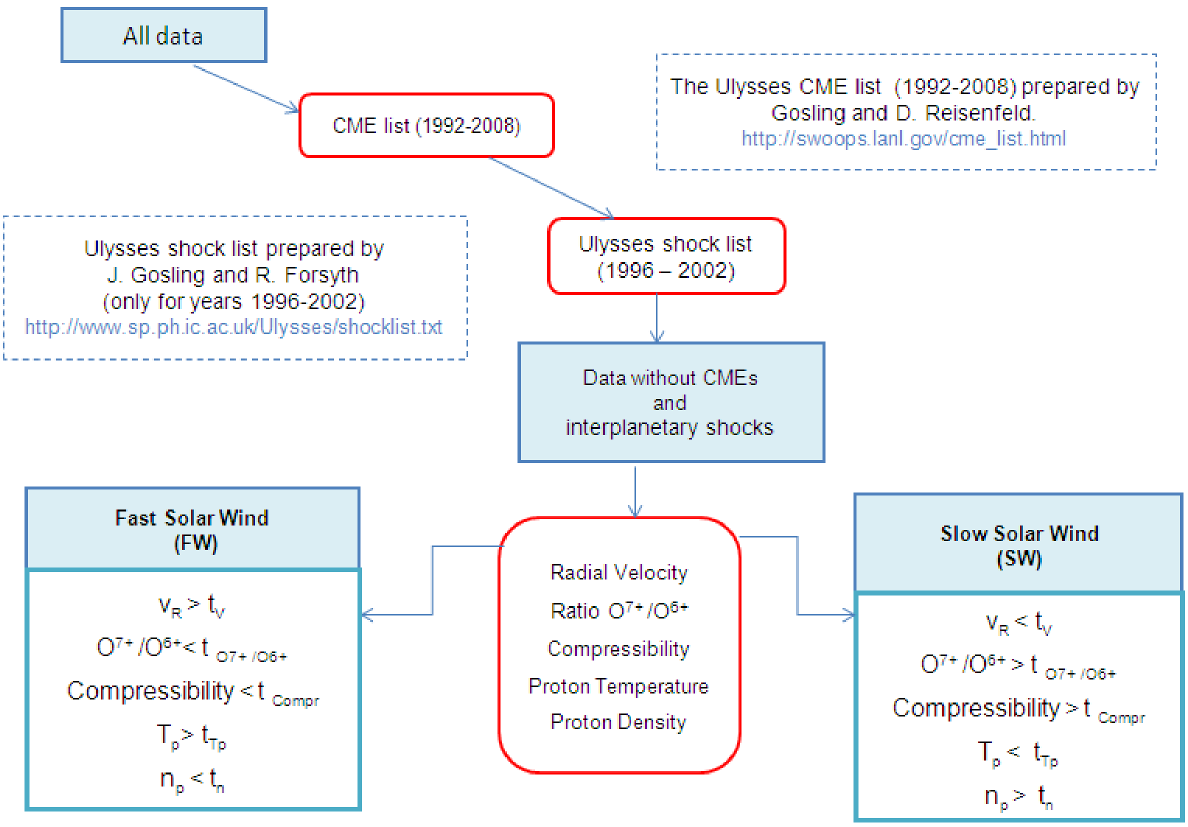

Figure 6.1: The logical flow chart for selection of “pure” fast and slow solar wind intervals from Ulysses data D5MINSW, D3MINSW, D1MAXSW databases.

Table 6.1: The threshold values applied to the five parameters used to select slow and fast solar wind streams in each year of three periods

Threshold	Solar Minimum		Solar Maximum			Solar Minimum	
	1997	1998	1999	2000	2001	2007	2008
	4.7-5.4 AU	5.2-5.4 AU	4.2-5.2 AU	2.0-4.2 AU	1.3-2.6 AU	1.4-2.6 AU	2.0-4.1 AU
t_V [km/s]	500	450	450	450	500	500	500
$t_{O7+/O6+}$	0.1	0.1	0.1	0.1	0.1	0.05	0.05
$t_{Compr.}$	0.1	0.1	0.1	0.1	0.1	0.1	0.1
t_{Tp} [K]	$5*10^4$(d<160) $4*10^4$(d>160)	$4*10^4$	$5*10^4$	$5*10^4$	$1*10^5$	$8*10^4$	$8*10^4$
t_n [cm^{-3}]	0.2	0.2	0.2	0.4 (d<200) 1.2 (d>200)	1.5	1.5	0.7 (d <200) 0.3 (d>200)
t_n [cm^{-3}] (at 1 AU)	5.2	5.7	4.5	4.9 (d<200) 7.5 (d>200)	5.7	6.0	5.1 (d<200) 4.2 (d>200)

We use 6-hour averages to select the threshold values for the five plasma and magnetic field parameters. As shown in Table 6.1, most of the threshold values vary with year and day of the year (reflecting change of heliocentric distance and heliolatitude). The five solar wind parameters and their associated scores were used to distinguish between the slow and fast streams. For each data sample we constructed a consolidated (final) score that specifies how many of the five individual scores are satisfied such that the sample can be classified as fast or slow wind. The consolidated score is formed by the sum of the 5 individual scores. Each individual score is equal to either 1 if the value of the corresponding parameter is larger than the threshold defined for fast wind or 0 otherwise (slow wind). If the consolidated/final score is equal to 4 or 5 we classify the sample as fast solar wind (FW). When the final score is equal to 0, 1 or 2 the sample is categorized as slow solar wind (SW). Cases when the score was 3 were disregarded from the analysis.

The figures 6.2-6.5 show how this selection procedure works on real Ulysses data, during solar maximum (Fig. 6.2, 6.3) and solar minimum (Fig. 6.4, 6.5). The plots show the five individual scores and the final score that is used for final selection of the sample as fast or slow solar wind.

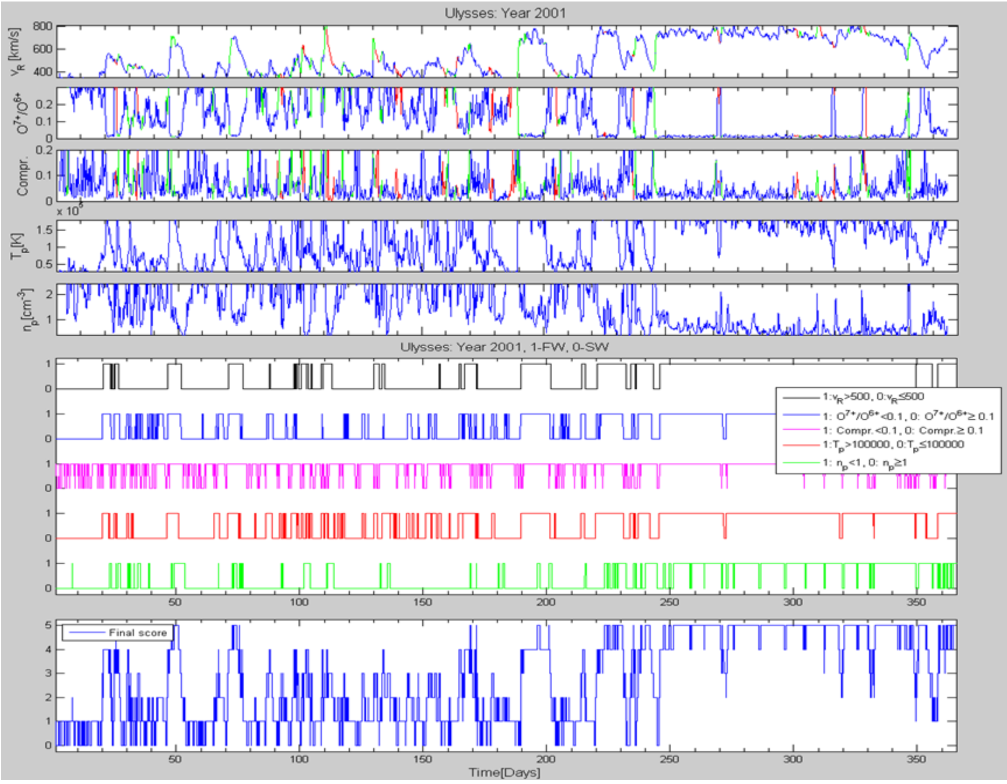

Figure 6.2: (a) The five selected solar wind parameters in 2001 (solar maximum); (b) the corresponding individual scores; (c) the final score specifying how many of the five individual scores are satisfied. When the final score equals 4 or 5 identify the sample is considered as fast solar wind (FW), while values 0, 1 or 2 designate slow solar wind (SW).

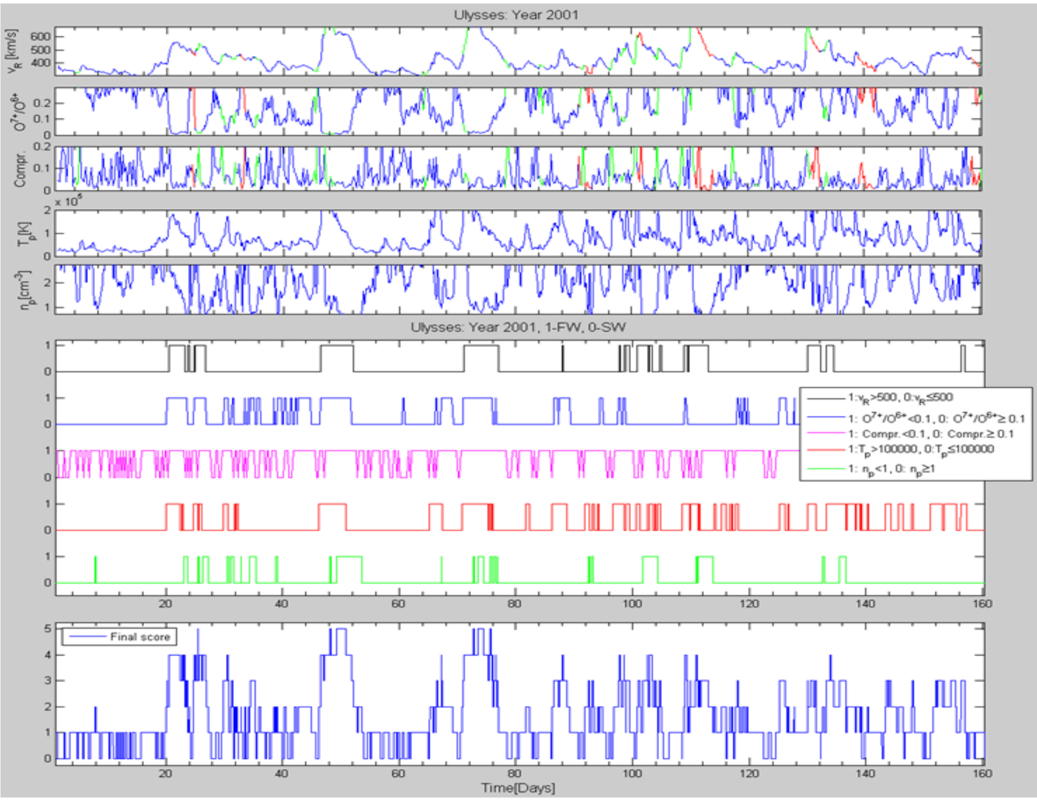

Figure 6.3: The same as Figure 6.2 for days 1 – 160 in 2001.

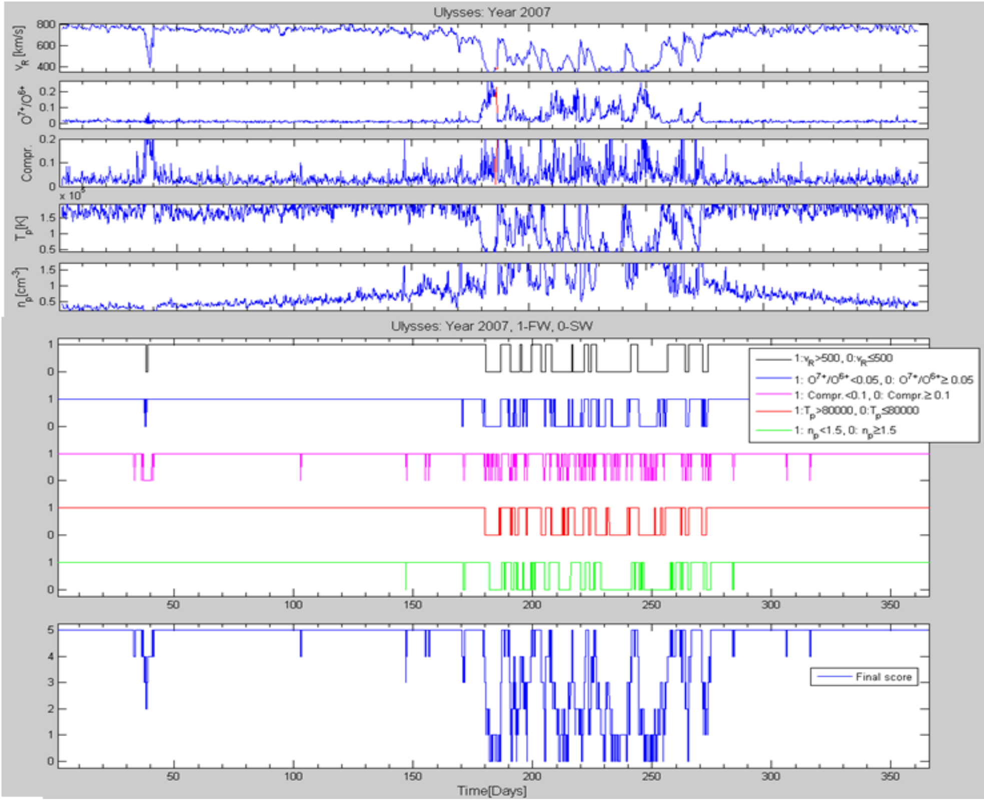

Figure 6.4: The same as Figure 6.2 for the year 2007.

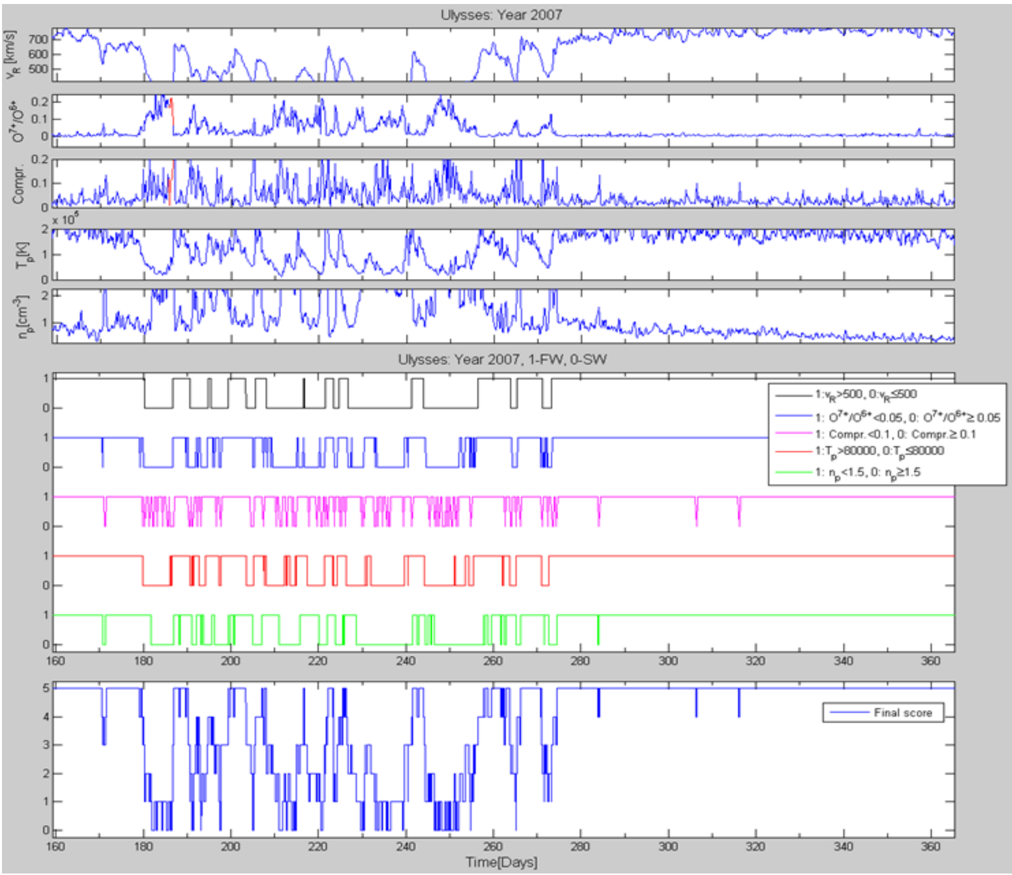

Figure 6.5: The same as Figure 6.2 for days 160 – 365 in 2007.

Based on the final score, we identified 46 time intervals of fast solar wind and 43 time intervals of slow solar wind. The information on these data is stored into an excel file, where, in addition to the information about final scores and basic characteristics, we have also included the information about the number of samples and data gaps for each interval. This file (Ulysses_data_selection.xls) is available in the ftp repository together with the catalog.

As Figure 6.6 shows, there are some very long fast solar wind intervals originating from large polar coronal holes (especially in 2007). In order to avoid that the changing radial distance of Ulysses affects the solar wind parameters (especially the density), we restricted the maximum interval length in PSD calculation to one week. (Note also that the data after 15^{th} of January 2008 had to be neglected because of insufficient data quality).

The final number of slow and fast solar wind intervals used for PSD calculation are the following:

In 1997-1998 (D5MINSW) 12 slow wind and 5 fast wind intervals.
In 1999-2001 (D1MAXSW) 27 slow solar wind and 32 fast wind intervals.
In 2007-2008 (D3MINSW) 4 slow wind and 9 fast wind intervals.

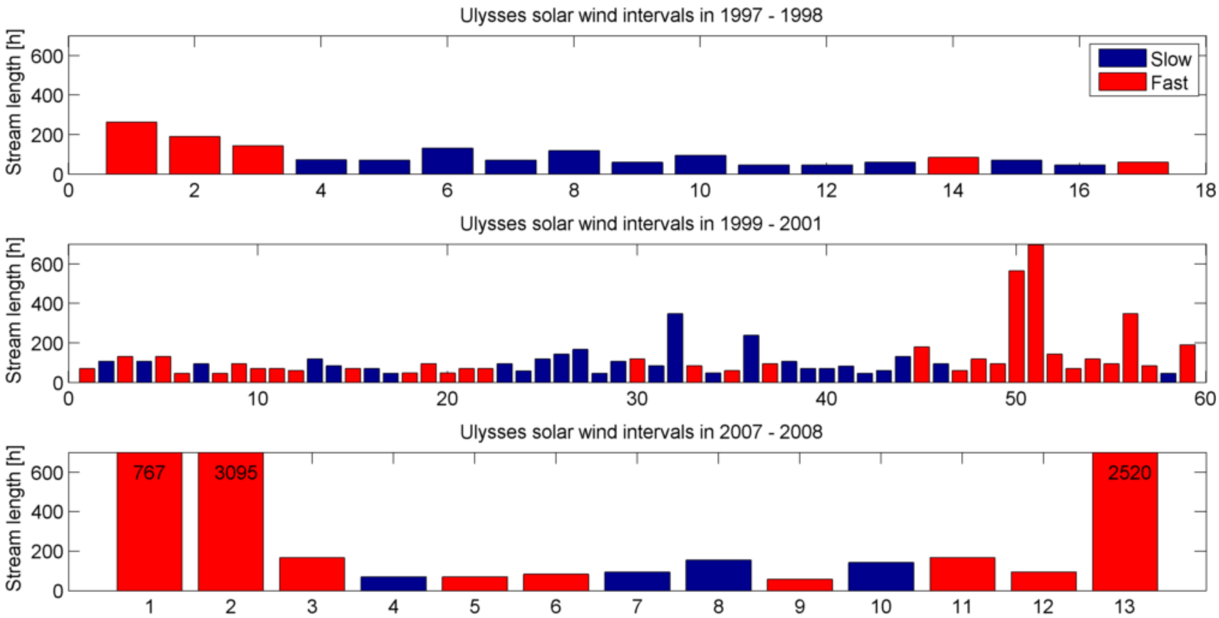

Figure 6.6: Lengths of the selected slow and fast solar wind intervals of Ulysses data. Intervals are ordered according to their times in each period.

6.2 Cluster

We use data from Cluster 1 and 3 (separately when calculating the PSDs) since these two spacecraft offer sufficient instrumentation for data selection. In order to select only undisturbed solar wind we have to exclude from the data intervals the time periods when Cluster encounter the ion and electron foreshocks . The ion foreshock effects are identified as time intervals when the flux (F_E) of

the highest energy channels (about 6 – 30 keV) of CIS-HIA instrument exceeds the threshold specified in Table 6.2. In order to exclude the electron foreshock we reject intervals in which the wave energy (E) measured by WHISPER exceeds the threshold of Table 6.2 .

These criteria for selecting the solar wind intervals "contaminated" by magnetospheric ions and electrons can only be applied when there are simultaneous measurements available in CAA for the five parameters: spacecraft position, magnetic field magnitude, ion velocity, omni-directional ion energy flux and wave energy density. This sets additional limits to the number of solar wind intervals.

Table 6.2: Thresholds for selecting " pure" solar wind from Cluster measurements.

Threshold Year	$\mathbf{X}_{GSE}$ R_E	$\lvert\mathbf{B}_{GSE}\rvert$ nT	$\mathbf{F}_E$ keV cm^{-2} s^{-1} sr^{-1} keV^{-1}	**E** V^2 m^{-2} Hz^{-1}
2001	> 0	< 20	$< 1*10^5$	$< 1*10^{-12}$
2007	> 0	< 20	$< 1*10^5$	$< 1*10^{-12}$
2008	> 0	< 20	$< 1*10^5$	$< 1*10^{-14}$

After finding the pure solar wind intervals, they are divided into fast (V > 450 km/s) and slow (V < 450 km/s) wind intervals.

In 2001 (D1MAXSW) we find 21 slow wind and 1 fast wind intervals from Cluster 1 and 20 slow wind intervals from Cluster 3. In 2007-2008 (D3MINSW) we find 57 slow wind and 18 fast wind intervals from Cluster 1 and 47 slow wind and 7 fast wind intervals from Cluster 3.

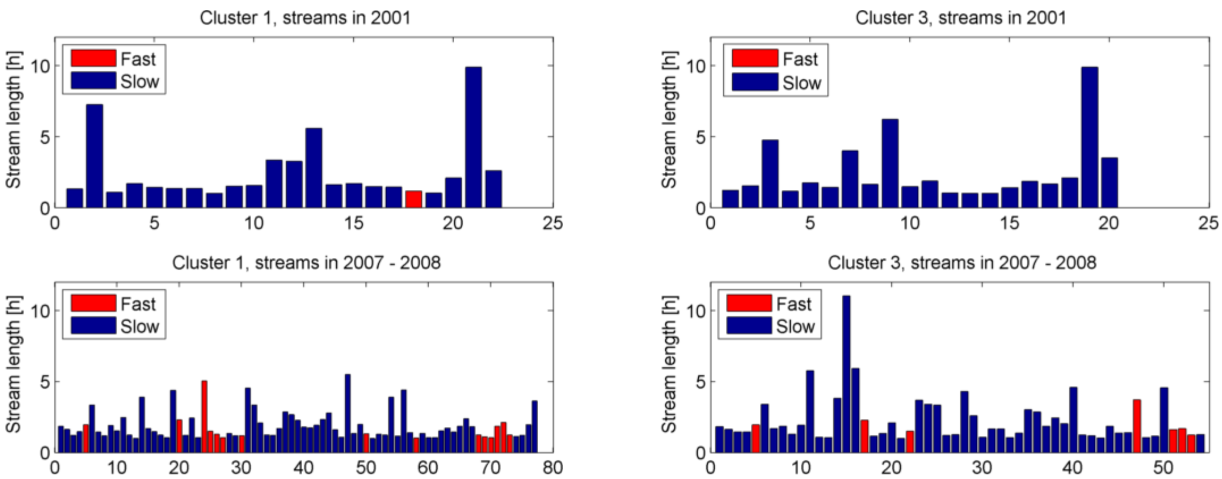

Figure 6.7: Lengths of slow and fast solar wind intervals of Cluster 1 (left) and 3 (right) data. Intervals are ordered according to their times in each period.

6.3 Venus Express

VEX solar wind data selection is based on the plasma bulk velocity measured by ASPERA at a resolution of 196 seconds. The contamination of solar wind by Venusian ion foreshock is virtually zero because, on the one hand, Venus has no intrinsic magnetic field, thus the induced magnetosphere is quite small and the foreshock size is reduced accordingly (Crawford et al., 1993) and, on the other hand, ASPERA is switched on for time intervals of the order of one hour only, close to the orbital apogee, more than 50000 kilometers away from Venus (see Figure 6.8). We used a selection threshold for fast solar wind consistent with the one defined for Cluster at 1 AU (see Table 6.3), for the same time interval, 2007-2008, i.e. we consider the sample is fast solar wind if the velocity is larger than 450 km/s. We included only those time intervals larger than one hour that do not have data gaps longer than 30 seconds. VEX intersected a total of 29 fast solar wind intervals in 2007 - 2008 (16 in 2007 and 13 in 2008).

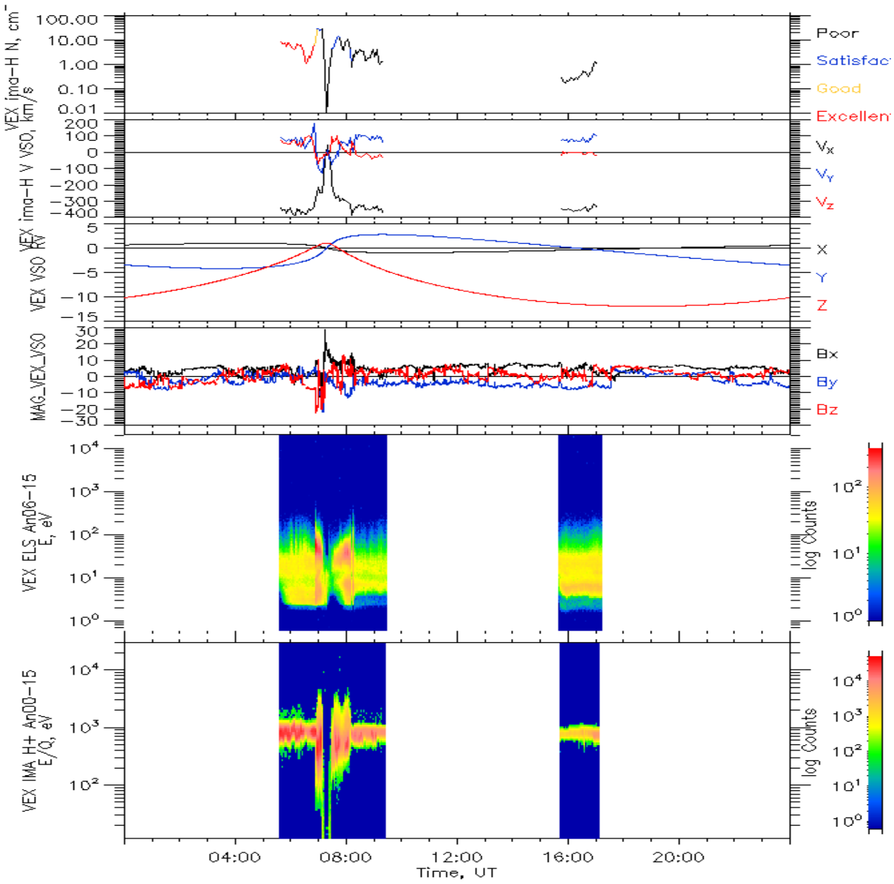

Figure 6.8: : Example of VEX data (30/01/2007 from the AMDA database. Panels from top: the proton density; three components of the proton velocity in VSO coordinate system; spacecraft position (x,y,z) in Venus radii; three components of magnetic field in VSO system; proton energy spectrum; electron energy spectrum. Note that the first time interval (05:40 UT - 09:15 UT) of ion and electron data includes the passage through Venus magnetosheath and induced magnetosphere, while only the second one (15:45 UT - 17:05 UT) corresponds to the pure solar wind.

Table 6.3: Thresholds for selecting fast wind from Venus Express measurements.

Threshold Year	$\mathbf{Z}_{VSO}$, km	$\lvert\mathbf{V}_{fast\ wind}\rvert$ km/s
2007	> 40000	> 450
2008	> 40000	> 450

7. Welch method for PSD calculation

The estimation of the Power Spectral Density (PSD, sometimes called periodogram) of a signal $x(t)$ is a central issue of time series analysis (Oppnheim & Schafer, 1975). In the course of the years, different methods have been developed to achieve this estimation. Given a signal $x(n)$, sampled at a constant time rate $1/n$, the easiest way to estimate its PSD is to compute the Discrete Fourier Transform (DFT) of the signal:

$$\hat{X}(\omega) = \sum_{n=0}^{N-1} x(n) e^{-j\omega n}$$

where j is the imaginary unit, N is the number of points and ω is the angular frequency ($\omega = 2\pi/T$ where T is the period).The PSD is proportional to the squared Fourier amplitude:

$$S_N(\omega) = \frac{1}{N}\left|\hat{X}(\omega)\right|^2$$

This *periodogram*, represents a rough estimate of the PSD, but may sometimes include a large error. Indeed, the error in estimating the PSD as described above is

$$\sigma^2\left(S_N(\omega)\right) = \sigma^4{}_x\left[1 + \left(\frac{\sin(\omega N)}{N \sin \omega}\right)^2\right] \cong S_N^2(\omega)\left[1 + \left(\frac{\sin(\omega N)}{N \sin \omega}\right)^2\right]$$

where σ^2 is the variance of the PSD.

A way to reduce the error in estimating the PSD was introduced by Bartlett (1948) and consists in averaging a large number of PSD estimations. This is done by partitioning the original timeseries $x(n)$ of length N in a set of K consecutive (adjacent) segments of length $M=N/K$, then computing the PSD for each segment and finally averaging the obtained PSDs,

$$S^B(w) = \frac{1}{KM}\sum_{i=1}^{k}\left|\hat{X}_M(w)\right|^2$$

Proceeding in this way clearly reduces the error (variance) by a factor *K*.

Welch method (1967) is a variant of the Bartlett's method. Differently from Bartlett's method, Welch method allows a certain superposition of the segments in which the timeseries is partitioned. In other words, in Welch's method the segments are no longer adjacent but can be superposed up to a certain percentage. Successively, a window is applied to each segment to reduce the end-effects before computing the individual segment PSDs. Finally, the PSD of the original signal *x*(*n*) is computed by averaging the set of the PSDs computed for the segments. Since the number of segments in Welch method is generally larger than in Bartlett's method, the error in estimating the PSD is lower. However, because of the superposition of segments, the PSDs of each segment are no longer independent as they are for Bartlett's method.

8. PSD calculation

The window used in computing the PSD Welch method is the well-known *Hanning window*, (see also Figure 8.1):

$$w(n) = \frac{1}{2}\left(1 - \cos\left(\frac{2\pi n}{N-1}\right)\right)$$

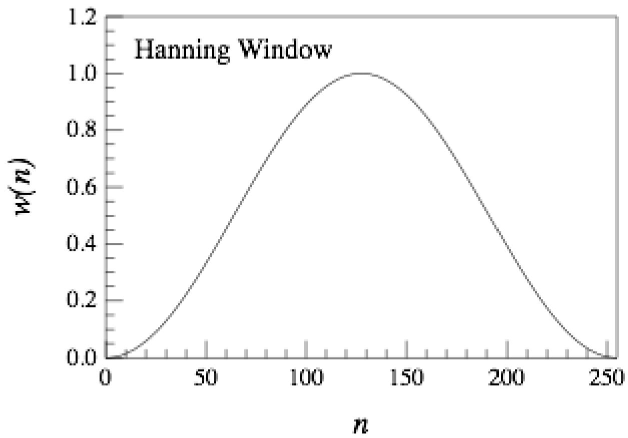

Figure 8.1. The shape of the Hanning window for N = 250.

To show the effect of applying a Hanning window to PSD estimation by Welch's method, we show in Figure 8.2 the results obtained when using a square and a Hanning window for a Gaussian white noise (panel a) and for an Ornstein-Uhlenbeck (OU) noise [Uhlenbeck and Ornstein, 1930] (panel b) generated using the following map:

$$x(n+1) = \left(1 - \frac{1}{\tau}\right)x(n) + \eta(n)$$

where τ is a correlation time and η is a de-correlated white noise.

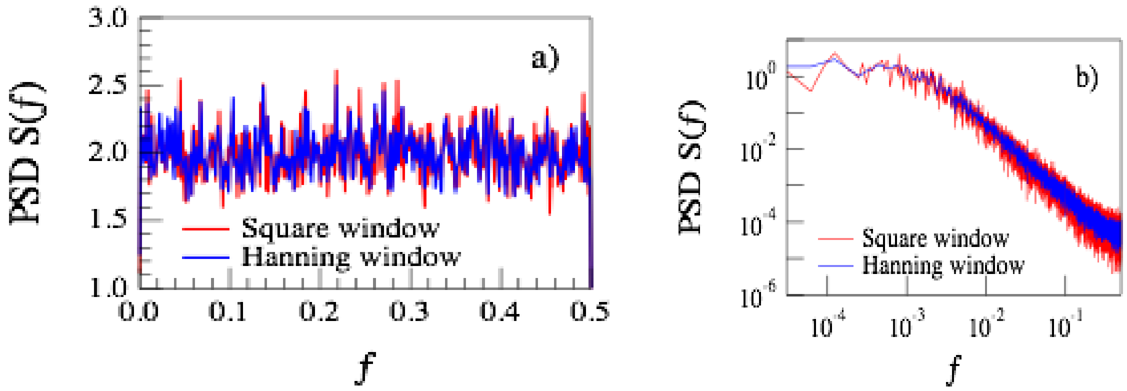

Figure 8.2. Effect of windowing on PSD estimation by Welch method. Panels a) and b) refer to Gaussian white noise and Ornstein-Uhlenbeck -noise, respectively. Used window are the square (red) and Hanning (blue) windows. Hanning window results to lower noise.

The effect of increasing the number of segments (*K*) in Welch algorithm is shown in Fig. 8.3. The PSDs shown in Fig. 8.3 were computed for a Gaussian white-noise signal of 524288 elements. The sampling time was 1 s. As expected, the PSDs become less noisy when the number of segments is increased. Thus, segmentation helps in interpreting spectra and in finding the best spectral model to be fitted. On the other hand, it is also notable that the increasing number of segments results in the shortening of the time-series for which periodograms are computed. This weakens the frequency resolution of the final averaged PSD and raises the limit of lowest frequency attained see also Fig. 8.3. The smaller frequency resolution can also weaken the accuracy and reliability of the fitted spectral model (power-law, in most cases).

Summarizing, the computation of PSDs according to Welch method reduces the error of the obtained spectra, but also reduces the frequency resolution of the periodograms. The latter feature means that the spectral information contained in the investigated signal is not fully exploited in Welch method. Spectral information weakens with the increasing number of segments, which is especially important when the analyzed signal is short, like e.g. in the case of solar wind intervals of the Cluster mission. Therefore, the number of segments should be adjusted to the length of the analyzed time-series.

In case of Cluster and VEX, the fast/slow solar wind intervals typically last from one hour to ten hours but in Ulysses we defined the longest intervals to span one week. In order to make results more comparable we used a rather short segment length of 12 hours for Ulysses and a fixed segment length of 25% from the interval length for Cluster. The overlap was 50% for both. For VEX we used segment length of 8.5 minutes and 90% overlap.

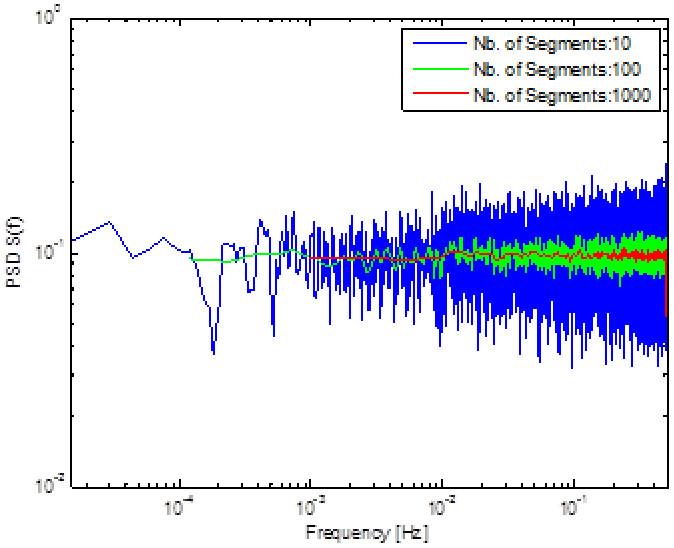

Figure 8.3. Power spectral density function of a Gaussian white-noise signal of 524288 elements computed according to Welch method. Blue, green and red curves correspond to the spectra obtained when using 10, 100 or 1000 segments (see text), respectively.

9. Description of the catalog of PSDs for solar wind data

The PSD catalog is organized as an ftp repository integrated into the website of the project at http://www.storm-fp7.eu. The structure of the ftp repository is defined according to the guidelines stated in the Grant Agreement and its main pillars are the three databases: D5MINSW between 1997-1998 (includes Ulysses data and PSDs), D1MAXSW between 1999 - 2001 (includes Ulysses and Cluster data and PSDs) and D3MINSW between 2007-2008 (includes Ulysses, Cluster and Venus Express data). The folder for each interval contains PSD and Data folders for each satellite separately. The final satellite data, for which the PSDs are calculated, are given in the Data folder, and the corresponding PSDs are in the PSD folder. Both of these folders are subdivided in satellite dedicated folders for those satellites that were operating during the respective interval. Finally, all the satellite folders were divided into folders of fast and slow wind. Figure 9.1 clarifies the folder structure of the catalog.

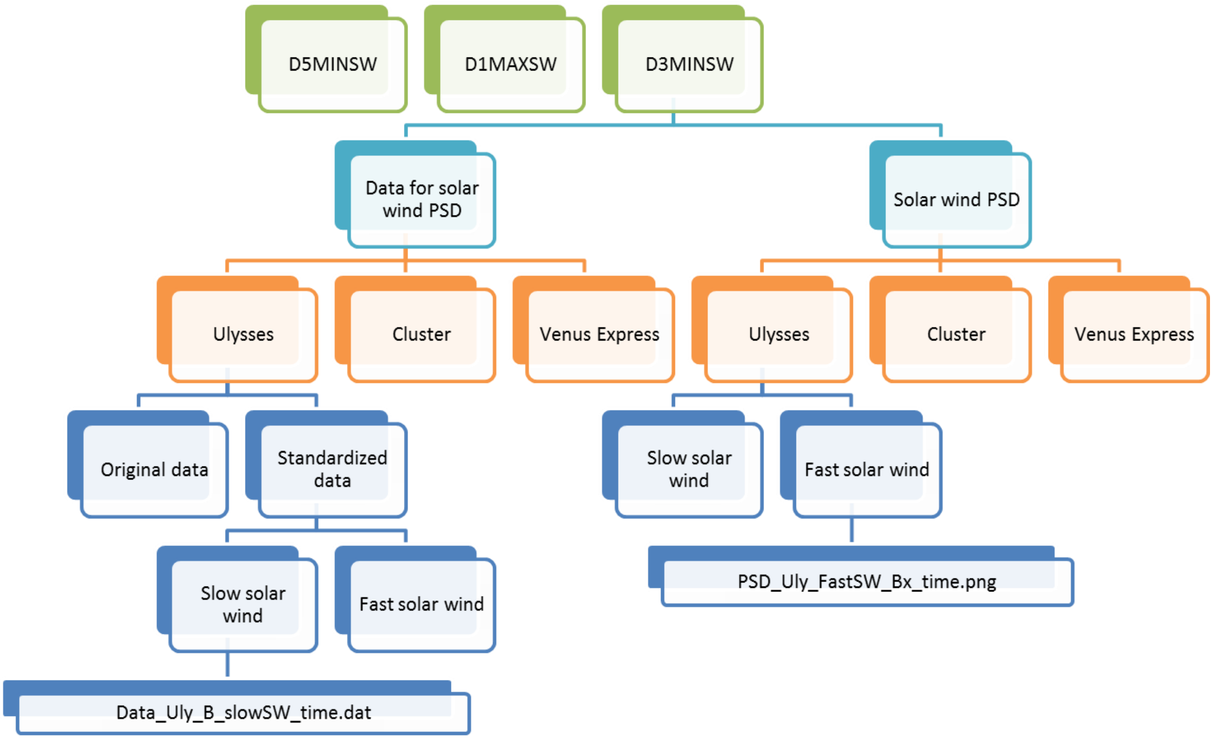

Figure 9.1. . Folder structure of the catalog (http://www.storm-fp7.eu).

There is one PNG figure file for each fast/slow solar wind intervals. The file is named according to figure type (PSD), satellite name (Uly, C1, C3, VEX), solar wind type (slowSW or fastSW), parameter (B_x, B_y, B_z, B^2, V_{sw}) and starting and ending hour of the data interval (yy_mm_dd_hh). For example: PSD_Uly_fastSW_B2_07_02_18_00-07_02_24_23.png. The PNG figure file contains a time series plot of the original satellite data and of the normalized (variance set to one) and detrended (linear trend removed) satellite data, as well as a plot of the power spectral density. Each Figure includes information about the length of the data interval, data coverage and the number of segments, the window type and the amount of overlap used in Welch method of PSD calculation. PSD spectral data (frequency and power) are also stored in separate txt-files in the same folder with the same file name as PNG figure.

Original satellite data is located in the folder "Original data", while the normalized and detrended data that is used to calculate the PSDs for Ulysses and Cluster satellites are in the "Standardized data" folder. Naming of standardized data files corresponds to the naming of PSD files for the same time interval.

Moreover, there is a separate outlier file in the Data folder of each satellite, showing timestamps of the removed outliers during the respective time interval.

Using Ulysses data we have included in the catalog 27 PSDs in D5MINSW (12 fast wind, 15 slow wind), 59 PSDs in D1MAXSW (33 fast wind, 26 slow wind) and 49 PSDs in D3MINSW (45 fast wind, 4 slow wind).

In D1MAXSW interval we have 22 PSDs using Cluster 1 data (1 fast wind, 21 slow wind) and 20 PSDs using Cluster 3 data (all slow wind). In D3MINSW interval we have 75 PSDs using Cluster 1 data (18 fast wind, 57 slow wind) and 54 PSDs using Cluster 3 data (7 fast wind, 47 slow wind).

VEX magnetic field data enabled computation of 374 PSD spectra (183 for 2007 and 191 for 2008) of which 110 PSD spectra correspond to fast wind streams (64 PSD spectra in 2007 and 46 PSD spectra in 2008).

10. Some examples of PSDs and preliminary scientific interpretation

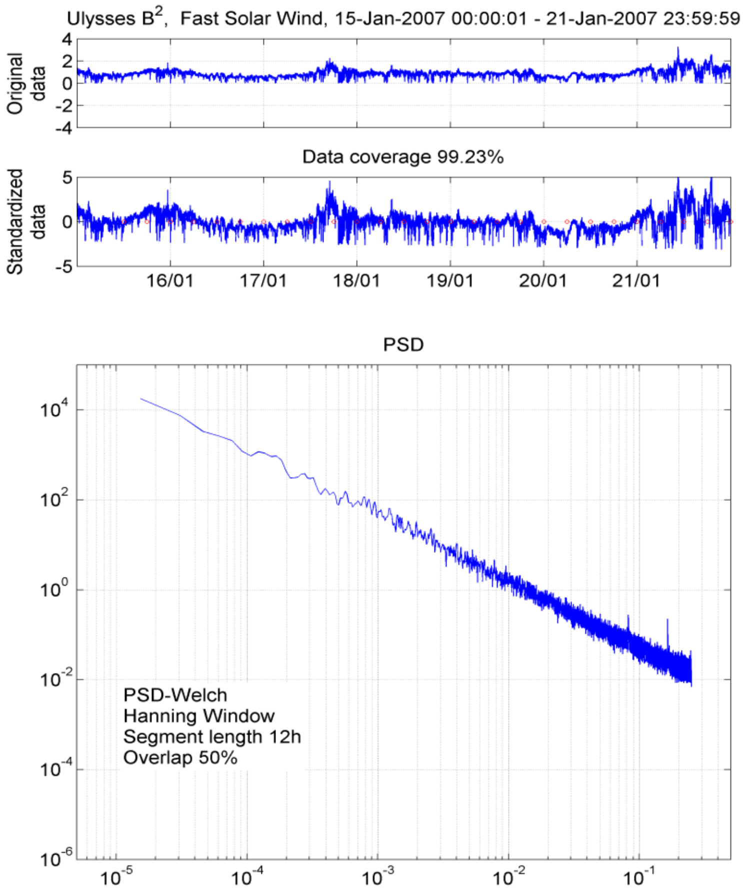

Figure 10.1. PSD for Ulysses squared magnetic field in fast solar wind stream and solar minimum conditions. Seven-day data interval starts at 15.1.2007 (PSD_Uly_fastSW_B2_07_01_15_00-07_01_21_23.png)

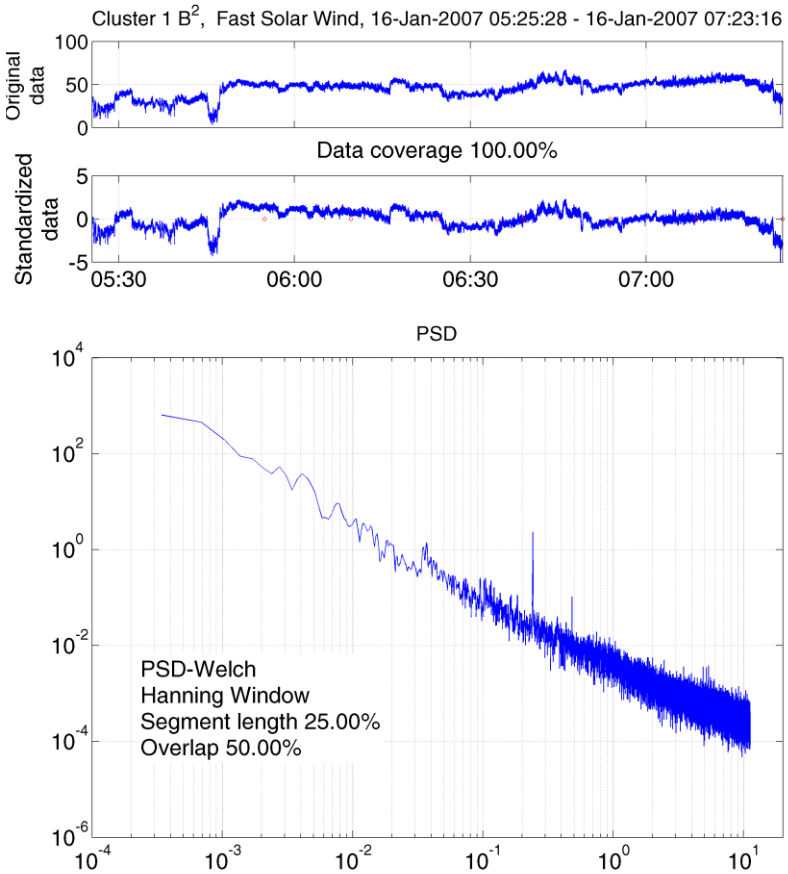

Figure 10.2. PSD for Cluster squared magnetic field in fast solar wind stream. Data interval occurs on 16.1.2007 (PSD_C1 _fastSW _B^2_07_01_16_05-07_01_16_07.png)

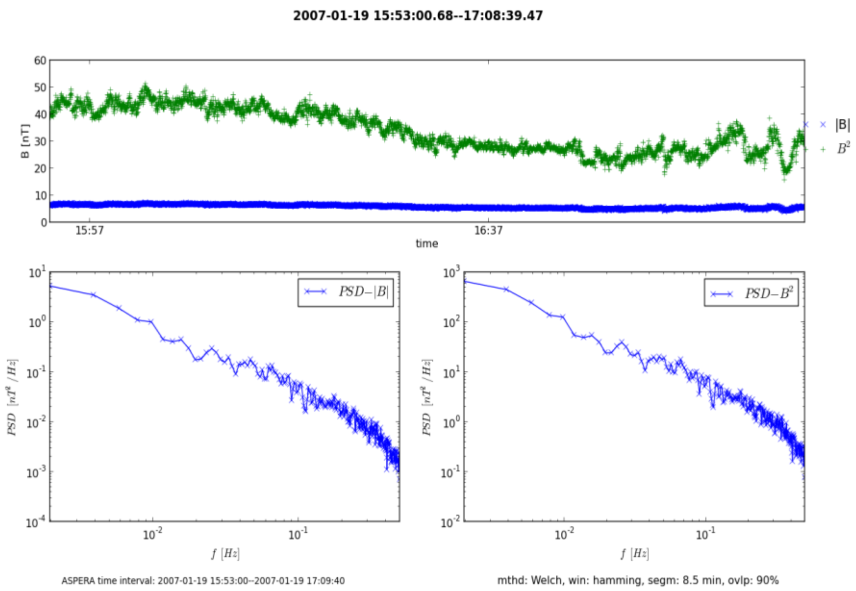

Figure 10.3. PSD for VEX magnetic field data on 19.1.2007, when the spacecraft encountered the fast stream seen earlier by Cluster on 16.01.2007.

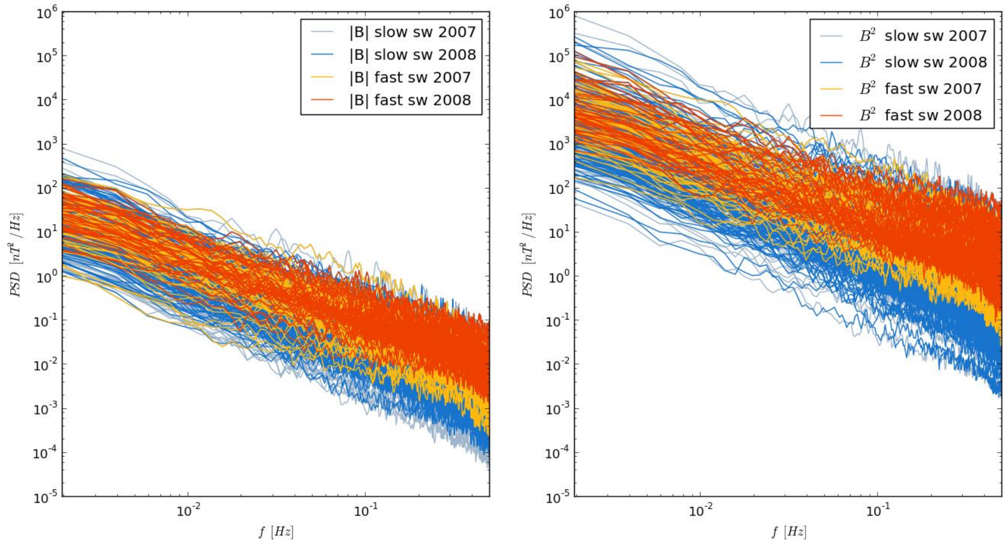

Figure 10.4. Summary plot of the 374 PSD spectra for VEX magnetic field included in the D3SWMIN database. Left panel: total magnetic field; right panel: $|B|^2$. Light and deep blue are used for slow wind in 2007 and 2008; yellow and red for fast wind in 2007 and 2008. Fast wind intervals are defined as those intervals for which the plasma bulk velocity is larger than 450 km/s. Everything else is considered slow, thus it is possible that some slow wind intervals include transition regions like Corrotating Interaction Regions (CIR) or trailing edges of fast streams. Plasma data on board VEX do not enable further investigation of the origin of the solar wind.

It is for the first time when the spectral properties of turbulence are analyzed systematically at 0.72 AU during solar minimum conditions. From this point of view, and in spite of difficult measurement conditions, the contribution of VEX to STORM and generally to the investigation of solar system plasma turbulence is quite unique. The preliminary analysis of PSD spectra from Venus Express reveals at least three important facts:

1. A power law regime is observed in the frequency range [10^{-3} Hz, $2*10^{-1}$ Hz] that would correspond to the smallest scales of the solar wind inertial range. Due to the limited time range of VEX observations in the solar wind this is indeed a very limited range of scales, nevertheless comparison with PSD from Ulysses and Cluster during the same time intervals, particularly for high speed streams, could provide additional data;
2. A decreasing of the spectral power seems to be observed while the solar minimum deepens (see figure 10.4); also the power over all frequencies is larger for fast streams;
3. There are consistent and systematic observations of a spectral break at roughly $3*10^{-1}$ Hz; further investigation is needed to understand whether this feature of VEX PSDs in the solar wind is related to a change of the turbulence regime, possibly a new inertial range or a hallmark of the dissipation range, or is partially determined by instrumental effects/noise.

11. References

Balogh, A., Beek, T. J., Forsyth, R. J., Hedgecock, P. C., Marquedant, R. J., Smith, E. J., The magnetic field investigation on the ULYSSES mission - Instrumentation and preliminary scientific results,

Astronomy and Astrophysics Supplement Series, vol. 92, no. 2, p. 221-236, 1992

Balogh, A.; Dunlop, M. W.; Cowley, S. W. H.; Southwood, D. J.; Thomlinson, J. G.; Glassmeier, K. H.; Musmann, G.; Luhr, H.; Buchert, S.; Acuna, M. H.; Fairfield, D. H.; Slavin, J. A.; Riedler, W.; Schwingenschuh, K.; Kivelson, M. G., The Cluster Magnetic Field Investigation, Space Science Reviews, v. 79, Issue 1/2, p. 65-91, 1997

Barabash, S., J.-A. Sauvaud, H. Gunell, et al., The Analyser of Space Plasmas and Energetic Atoms (ASPERA-4) for the Venus Express mission, Planetary and Space Science 55, 1772–1792, 2007

Bartlett, M.S., Smoothing Periodograms from Time-Series with Continuous Spectra, Nature, 161, 686, 1948

Bruno, R., Carbone, V., The Solar Wind as a Turbulence Laboratory, Living Reviews in Solar Physics, vol. 10, no. 2, 2013Crawford, G.K., Strangeway, R.J., Russell, C.T., VLF emissions in the Venus foreshock - Comparison with terrestrial observations , Journal of Geophysical Research , 98, no. A9, p. 15,305-15,317, 1993

P. M. E. Décréau[1], P. Fergeau[1], V. Krasnoselskikh[1], E. Le Guirriec[1], M. Lévêque[1], Ph. Martin[1], O. Randriamboarison[1], J. L. Rauch[1], F. X. Sené[1], H. C. Séran[1], J. G. Trotignon[1], P. Canu[2], N. Cornilleau[2], H. de Féraudy[2], H. Alleyne[3], K. Yearby[3], P. B. Mögensen[4], G. Gustafsson[5], M. André[5], D. C. Gurnett[6], F. Darrouzet[7], J. Lemaire[7], C. C. Harvey[8], P. Travnicek[9], and Whisper experimenters, Early results from the Whisper instrument on Cluster: an overview, Ann. Geophys., 19, 1241-1258, 2001

Erdös, G., and A. Balogh, Magnetic Flux Density Measured in Fast and Slow Solar Wind Streams, The Astrophysical Journal, 753, 130, 2012.

Lepri, S. T.; Landi, E.; Zurbuchen, T. H., Solar Wind Heavy Ions over Solar Cycle 23: ACE/SWICS Measurements, The Astrophysical Journal, Volume 768, Issue 1, article id. 94, 13 pp., 2013

Bame, S. J., McComas, D. J., Barraclough, B. L., Phillips, J. L., Sofaly, K. J., Chavez,, The ULYSSES solar wind plasma experiment, Astronomy and Astrophysics Supplement Series, vol. 92, no. 2, p. 237-265, 1992

McComas, D. J., R. W. Ebert, H. A. Elliott, B. E. Goldstein, J. T. Gosling, N. A. Schwadron, and R. M. Skoug, Weaker solar wind from the polar coronal holes and the whole Sun, Geophysical Research Letters, 35, 18,103, 2008.

Oppenheim, A.V., and R.W. Schafer, Digital Signal Processing, Prentice-Hall Inc., Englewood Cliffs, N.J., USA, 1975

Reme, H.; Bosqued, J. M.; Sauvaud, J. A.; Cros, A.; Dandouras, J.; Aoustin, C.; Bouyssou, J.; Camus, Th.; Cuvilo, J.; Martz, C.; Medale, J. L.; Perrier, H.; Romefort, D.; Rouzaud, J.; D`Uston, C.; Mobius, E.; Crocker, K.; Granoff, M.; Kistler, L. M.; Popecki, M.; Hovestadt, D.; Klecker, B.; Paschmann, G.; Scholer, M.; Carlson, C. W.; Curtis, D. W.; Lin, R. P.; McFadden, J. P.; Formisano, V.; Amata, E.; Bavassano-Cattaneo, M. B.; Baldetti, P.; Belluci, G.; Bruno, R.; Chionchio, G.; di Lellis, A.; Shelley, E. G.; Ghielmetti, A. G.; Lennartsson, W.; Korth, A.; Rosenbauer, H.; Lundin, R.; Olsen, S.; Parks, G. K.; McCarthy, M.; Balsiger, H., The Cluster Ion Spectrometry (cis) Experiment, Space Science Reviews, v.

79, Issue 1/2, p. 303-350, 1997

Smith, E. J., and A. Balogh, Decrease in heliospheric magnetic flux in this solar minimum: Recent Ulysses magnetic field observations, Geophys. Res. Lett., 35, L22103, 2008.

Uhlenbeck, G. E.; Ornstein, L. S. (1930). "On the theory of Brownian Motion". Phys. Rev. 36: 823–841. doi:10.1103/PhysRev.36.823

Wang, Y. -M, Robbrecht, E. and Sheeley, N. R. Jr. On the weakening of the polar magnetic fields during solar cycle 23. Astrophys. J, 707, 1372-1386, 2009.

Welch, P.D., The Use of Fast Fourier Transform for the Estimation of Power Spectra: A Method Based on Time Averaging Over Short, Modified Periodograms, IEEE Trans. Audio Electroacoustics, AU-15, 70, 1967

Zhang, T., Baumjohann, W., Delva, M., et al., Magnetic field investigation of the Venus plasma environment: Expected new results from Venus Express, Planetary and Space Science 54, 1336–1343, 2006

Yordanova, E.; Balogh, A.; Noullez, A.; von Steiger, R, Turbulence and intermittency in the heliospheric magnetic field in fast and slow solar wind, Journal of Geophysical Research, Volume 114, Issue A8, CiteID A08101, 2009